Acta Materialia

Effect of structural relaxation on crystal nucleation in glasses

--Manuscript Draft--

Manuscript Number:	A-20-2861
Article Type:	Full length article
Section/Category:	Opt in to First Look
Keywords:	nucleation; crystal growth; glasses; glass transition; general theory of phase transitions
Abstract:	Applying the Classical Nucleation Theory (CNT) to crystallization of glasses encounters some difficulties. One of the most important aspects is that this theory overlooks structural relaxation by assuming that crystal nucleation proceeds in a relaxed, metastable, supercooled liquid (SCL). Considering this assumption, the thermodynamic driving force, diffusion coefficient, and surface tension should be constant at any given temperature. Here, we performed experiments for very extended times (up to about 2,200 hours) at 703K, which well below the laboratory glass transition, [[EQUATION]] , of a lithium disilicate glass used as a model. Our results show that crystal nucleation starts concomitantly with the relaxation process of the glass towards the SCL, which strongly affects the nucleation kinetics, taking over 500 hours to reach the ultimate steady-state regime at this temperature. This very long relaxation is much slower than the well-known alpha relaxation process determining, e.g., the temporal evolution of the glass density, which takes only ~30 hours at this same temperature. Nevertheless, structural relaxation results in a decrease of the work of critical cluster formation leading to an upsurge of the nucleation rate. The increase of the nucleation rate mainly reflects this long structural relaxation mode of the glass and is not related to the classical transient nucleation, which has been exclusively employed in the interpretation of nucleation kinetics by most researchers, including ourselves, over the past 40 years. These experimental results and analyses prove that the theoretically predicted effect of glass relaxation on crystal nucleation, detailed in a forthcoming paper, is a well-founded possibility, and also sheds light on the alleged "breakdown" of the CNT at low temperatures.

Effect of structural relaxation on crystal nucleation in glasses

Vladimir M. Fokin[a], Alexander S. Abyzov[a,b], Nikolay S. Yuritsyn[c], Jürn W. P. Schmelzer[d], Edgar D. Zanotto[a]

[a]Department of Materials Engineering, Center for Research, Technology and Education in Vitreous Materials, Federal University of São Carlos, São Carlos, Brazil
[b]National Science Center Kharkov Institute of Physics and Technology, Kharkov, Ukraine
[c]Institute of Silicate Chemistry of Russian Academy of Sciences, nab. Makarova 2, 199034 St. Petersburg, Russia
[d]Institut für Physik der Universität Rostock, Albert-Einstein-Strasse 23-25, 18059 Rostock, Germany

Abstract

Applying the Classical Nucleation Theory (CNT) to crystallization of glasses encounters some difficulties. One of the most important aspects is that this theory overlooks structural relaxation by assuming that crystal nucleation proceeds in a relaxed, metastable, supercooled liquid (SCL). Considering this assumption, the thermodynamic driving force, diffusion coefficient, and surface tension should be constant at any given temperature. Here, we performed experiments for very extended times (up to about 2,200 hours) at 703K, which well *below* the laboratory glass transition, T_g, of a lithium disilicate glass used as a model. Our results show that crystal nucleation starts *concomitantly* with the relaxation process of the glass towards the SCL, which strongly affects the nucleation kinetics, taking over 500 hours to reach the ultimate steady-state regime at this temperature. This very long relaxation is much slower than the well-known alpha relaxation process determining, e.g., the temporal evolution of the glass density, which takes only ~30 hours at this same temperature. Nevertheless, structural relaxation results in a decrease of the work of critical cluster formation leading to an upsurge of the nucleation rate. The increase of the nucleation rate mainly reflects this long structural relaxation mode of the glass and is *not* related to the classical transient nucleation, which has been exclusively employed in the interpretation of nucleation kinetics by most researchers, including ourselves, over the past 40 years. These experimental results and analyses prove that the theoretically predicted *effect of glass relaxation on crystal nucleation*, detailed in a forthcoming paper, is a well-founded possibility, and also sheds light on the alleged "breakdown" of the CNT at low temperatures.

Keywords: Nucleation, crystal growth, glasses, glass transition, general theory of phase transitions

PACS numbers:

64.60.Bd General theory of phase transitions

64.60.Q Nucleation

64.70.Q Theory and modeling of the glass transition

70.kj Glasses

1. Introduction

Understanding the intricacies of the mechanisms and kinetics of crystallization of glass-forming liquids is vital for numerous scientific and technological reasons. Straightforward arguments are that the knowledge of crystal nucleation and growth rates is an essential requirement for avoiding crystallization during glass making [1] or controlling the crystallization process for glass-ceramic development and industrial production [2].

The Classical Nucleation Theory (CNT) is a popular tool used for analyzing or predicting nucleation rates in glass-forming liquids as a function of time, temperature or pressure. According to the CNT, crystallization takes place via stochastic thermal fluctuations in a supercooled liquid resulting in the formation of crystal nuclei of supercritical sizes followed by spontaneous, deterministic growth [3, 4]. CNT gives a very good description of the steady-state nucleation rates, $I_{st}(T)$, for temperatures above the temperature T_{max} of the experimentally observed maximum of the nucleation rate, $I_{st}(T_{max})$. For silicate glass-forming melts, this maximum has been reported to occur at $T_{max}/T_m \approx 0.55 - 0.65$, where T_m is the melting temperature.

However, at $T < T_{max}$ the theoretically predicted steady-state nucleation rates (from fitting to experimental data above T_{max}) *exceed* the values obtained in typical laboratory experiments, and this difference drastically increases with decreasing temperature. Some examples for different glass-forming systems [5-8] are shown in Fig. 1. This "breakdown" of CNT has been reported for different glass-forming systems, and various theoretical concepts have been advanced to explain it [6,9-11]. In [12,13] the problem of "breakdown" was analyzed in the terms of non-stationary nucleation, assuming that the steady-state nucleation rate was not reached. Significant structural changes occurring in the glass and supercooled liquid in the glass transition interval and below have been hypothesized in [6,10,11].

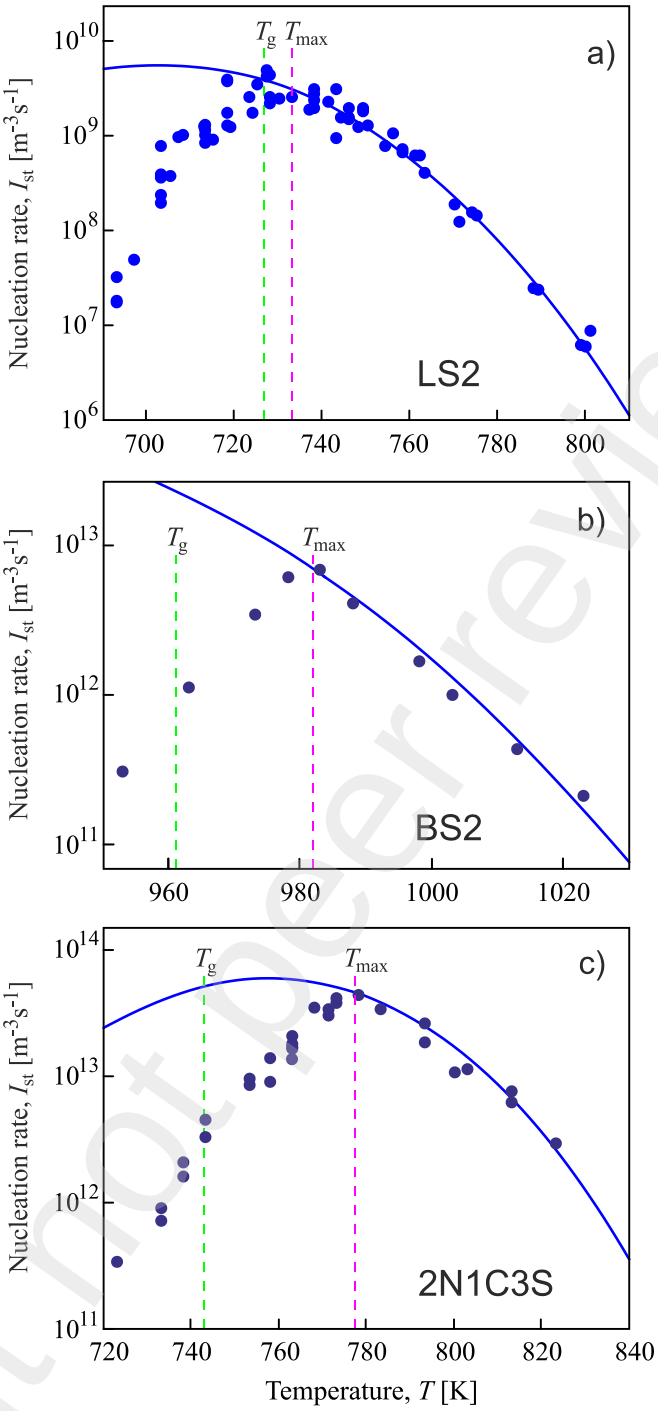

Fig. 1. Apparent "steady-state" nucleation rates for different glass-forming systems as a function of temperature [5-8] for: a) $Li_2O{\cdot}2SiO_2$ (LS2), b) $BaO{\cdot}2SiO_2$ (BS2), c) $2Na_2O{\cdot}1CaO{\cdot}3SiO_2$ (2N1C3S). The solid lines show the theoretically predicted steady-state nucleation rates by fitting the diffusion coefficient, $D(T)$, and the interfacial energy, $\sigma(T)$, of the CNT expression to the high temperature data, whereas the circles denote experimental values. They show the alleged break at T_{max}.

In the present work, we aim to find an explanation for the frequently reported break at low temperatures by analyzing another problem. The crucial question is: *Does the temporal evolution of the glass structure (relaxation or aging) significantly affect the crystal nucleation kinetics*? From a *theoretical* point of view, this problem, and also the possible influence of the melt history

on the crystallization behavior have already been analyzed in several publications [14-19], but were not solved. The possibility of explaining why this alleged "breakdown" at $T < T_{max}$ is so frequently reported, by taking into account the glass relaxation process, was briefly noted in [14]. However, to the best of our knowledge, a detailed *experimental* investigation of the *effects of structural relaxation on crystallization* has not been performed yet.

As a starting point, we would like to stress that crystal nucleation is very sensitive to changes in the glass structure. Temporal variations of the glass structure near the glass transition temperature, T_g, may significantly affect the nucleation kinetics. On the other hand, it is known [20-24] that the maximum steady-state nucleation rate usually measured in experiments is located near the glass transition interval. As a consequence, our premise to correlate such structural changes with the reported deviations between the theoretical predictions and experimental nucleation data receives additional support. A theory of the effects on crystal nucleation resulting from the glass transition and of structural changes caused by relaxation on nucleation, supplemented by a model analysis, are presented in [25].

In the present work, we attempt to solve the above formulated problem by an extensive analysis of experimental data obtained by significantly prolonging the nucleation times (up to 2,212 hours) as compared to those commonly used so far in typical nucleation experiments performed below T_g (< 100 hours). The materials used and methods adopted are described in Section 2. The results are presented in Section 3. An analysis and discussion are provided in Section 4. Some final remarks in Section 5 and a summary of the results and conclusion (Section 6) complete the paper.

2. Materials and Methods

Lithium disilicate glass was chosen for the present study because it shows bulk homogenous nucleation rates that are not too high or too low to be measured. There is enough thermodynamic information, which is required for the theoretical analysis of the experimental data, and a plethora of data on nucleation and growth rates are available for comparison purposes. The glass was synthesized using lithium carbonate (Alfa Aesar, USA, 99.0%) and quartz powder with a 20-30 μm particle size (Vitrovita, Brazil, 99.9%). Melting of the well-mixed reagents after a calcination stage at 1123 K for 15 h was performed in a platinum crucible for 4 h at 1673-1773 K. The melt was then poured onto a steel slab and pressed by a steel plate to vitrify it, forming 2.0-2.5 mm thick small broken pieces.

The glass transition temperature, T_g, was estimated by a differential scanning calorimeter (DSC 404, Netzsch, Selb/Bavaria, Germany) with a platinum pan and lid. The glass density was

determined at room temperature by hydrostatic weighting in kerosene after previous heat treatments for various times at $T = 703$ K and subsequent rapid cooling. The kerosene density was determined after each measurement of the sample density. Quartz glass (density 2.205 g/cm^3) was used as a reference. The accuracy was ± 0.001 g/cm^3. The isothermal evolution of the glass density at $T = 703$ K over time was used to estimate the classical alpha relaxation time.

The nucleation heat-treatments were performed in a vertical electric furnace with a pre-stabilized temperature kept constant within ± 1K. The small glass pieces were dropped into a support adequately placed inside the furnace, which yielded an estimated heating rate of 1,000 K/min. The number of crystals, *N*, that nucleated at temperature T in time t, were determined by the well-known "development" method proposed by Tammann [26] to grow the crystals to sizes visible under optical microscopes (NIKON ECLIPSE vv100n pol and Leica DMRX). To calculate *N* via the number of crystal sections on polished cross sections of the samples, we used stereological methods for the ellipsoidal LS2 crystals (see e.g. [27]). In the cases of very small *N*, which are typical for very short nucleation times, plane-parallel thin plates with polished sides were prepared for direct estimation of the crystal number in a given volume by transmitted light. Examples of transmitted and reflected light optical micrographs are shown in Fig. 2.

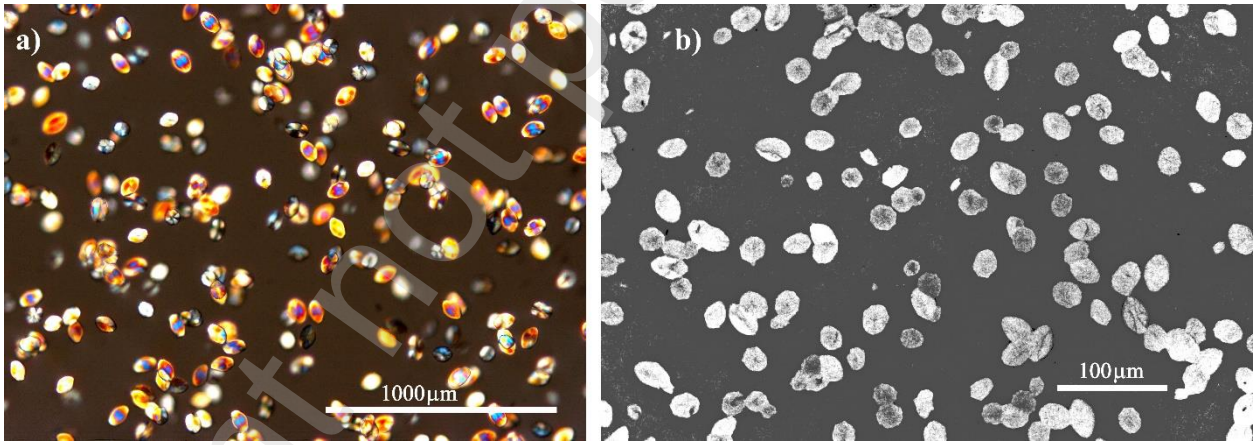

Fig. 2. a) Transmitted light micrograph of a 0.76 mm thick plate of a LS2 glass after nucleation at $T = 723$ K for 110 min and development at $T_d = 863$ K for 60 min. b) Reflected light micrograph of a cross-section of a LS2 glass sample after nucleation at $T = 746$ K for 3.5 h and development at $T_d = 863$ K for 17 min.

3. Results

Figures 3 - 8 show the number of crystals per unit volume versus time in glass samples subjected to nucleation temperatures, $T = 703$K, 713 K, 723 K, 738 K, 745 K, 758 K and 793 K, and then to a "development" treatment at $T_d = 863$ K. It should be noted that the maximum

nucleation times used here at 703K, 713K and 723K *exceeded by far* those typically used for lithium disilicate glass (e.g., [20]). The theoretical interpretation of these data is given in Section 4.

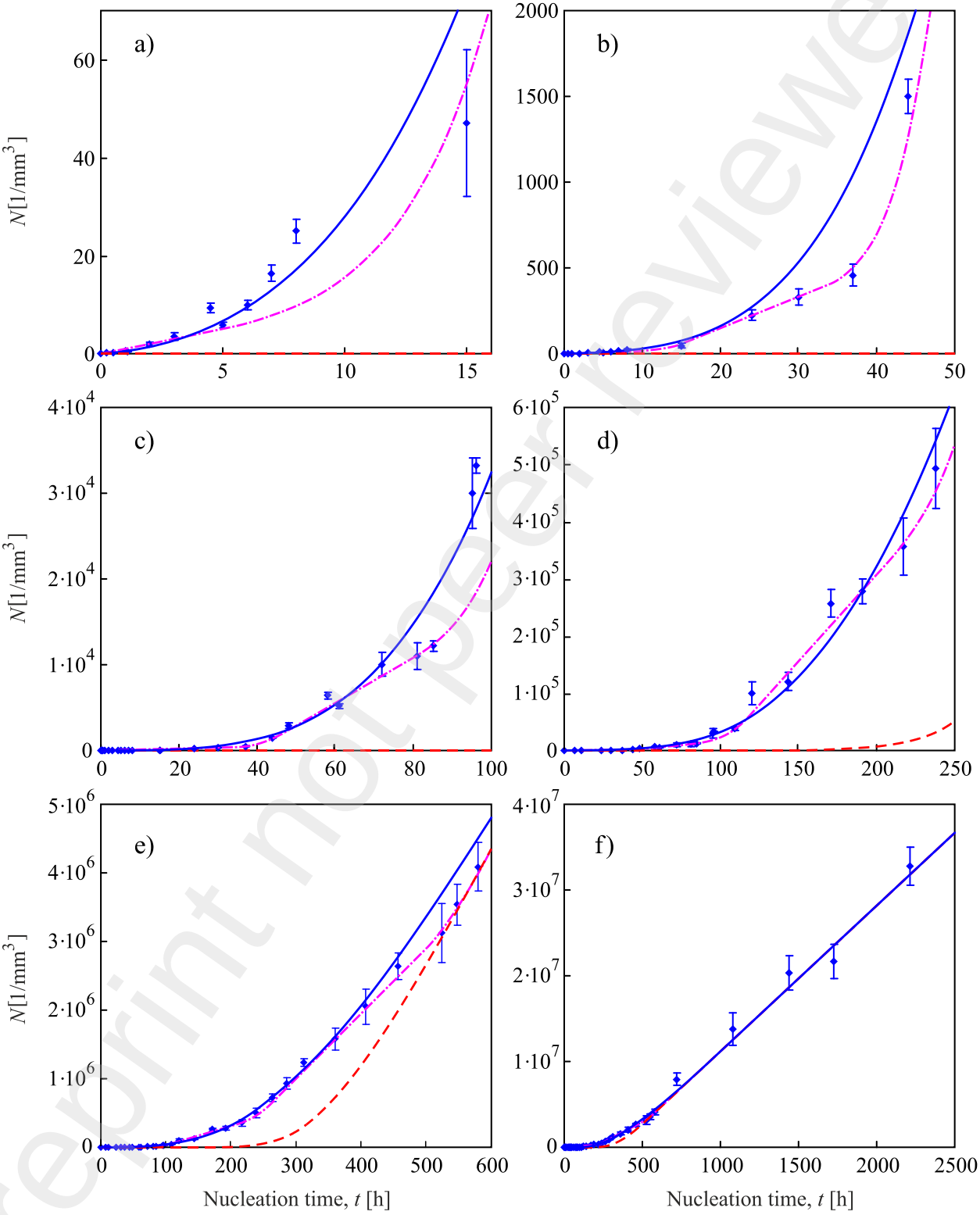

Fig. 3. Number of crystals per unit volume, $N(t)$, versus nucleation time, t, at $T = 703$ K for different time intervals. The dashed red lines were obtained via numerical simulations based on the *cluster dynamics* model with constant values of the diffusion coefficient, D, and surface tension, σ, which were determined as fitting parameters. The fitting procedure was performed to best

describe the *final part* of the $N(t)$-curve shown in Fig. 1f. The blue solid line shows a fit via Eqs. (14), (17), (18), whereas the magenta dashed-dotted line denotes a fit via Eqs. 14), (17), (18), (21), (22).

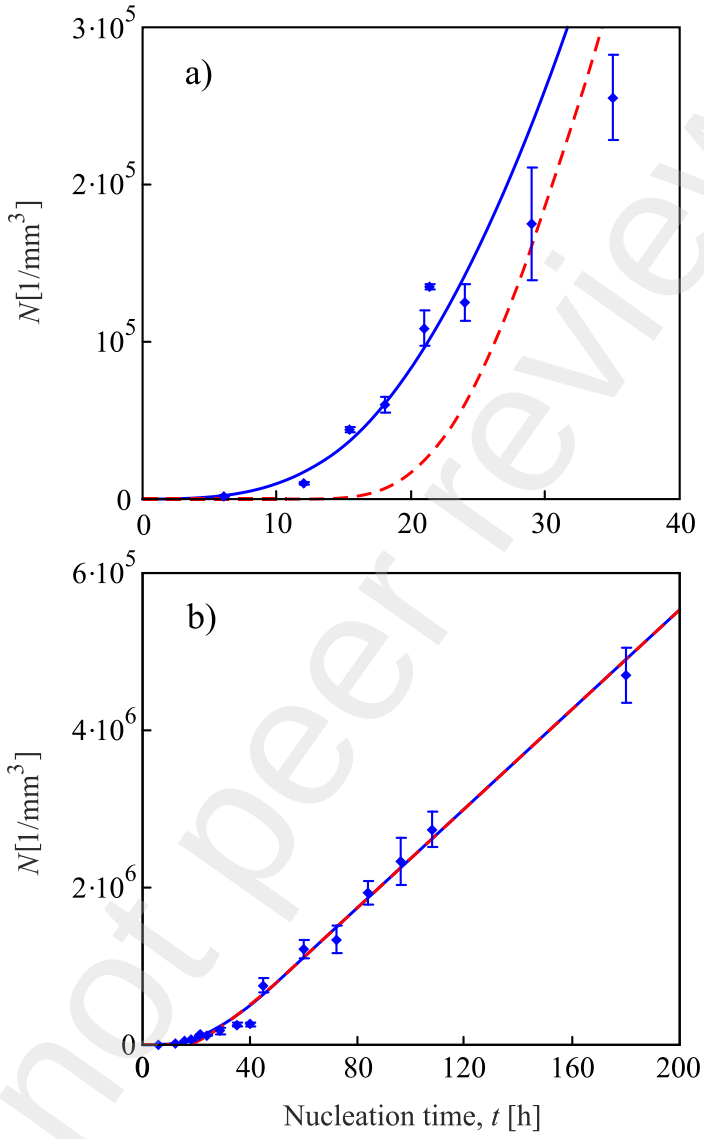

Fig. 4. Number of crystals per unit volume, $N(t)$, versus nucleation time, t, at $T = 713\text{K}$ for different time intervals. The dashed red lines were obtained via simulations based on the cluster dynamics model with constant D and σ, which are fitting parameters to best describe the *final linear part* of the $N(t)$ curve shown in Fig. 4b. The blue solid line denotes a fit via Eqs. (14), (17) and (18).

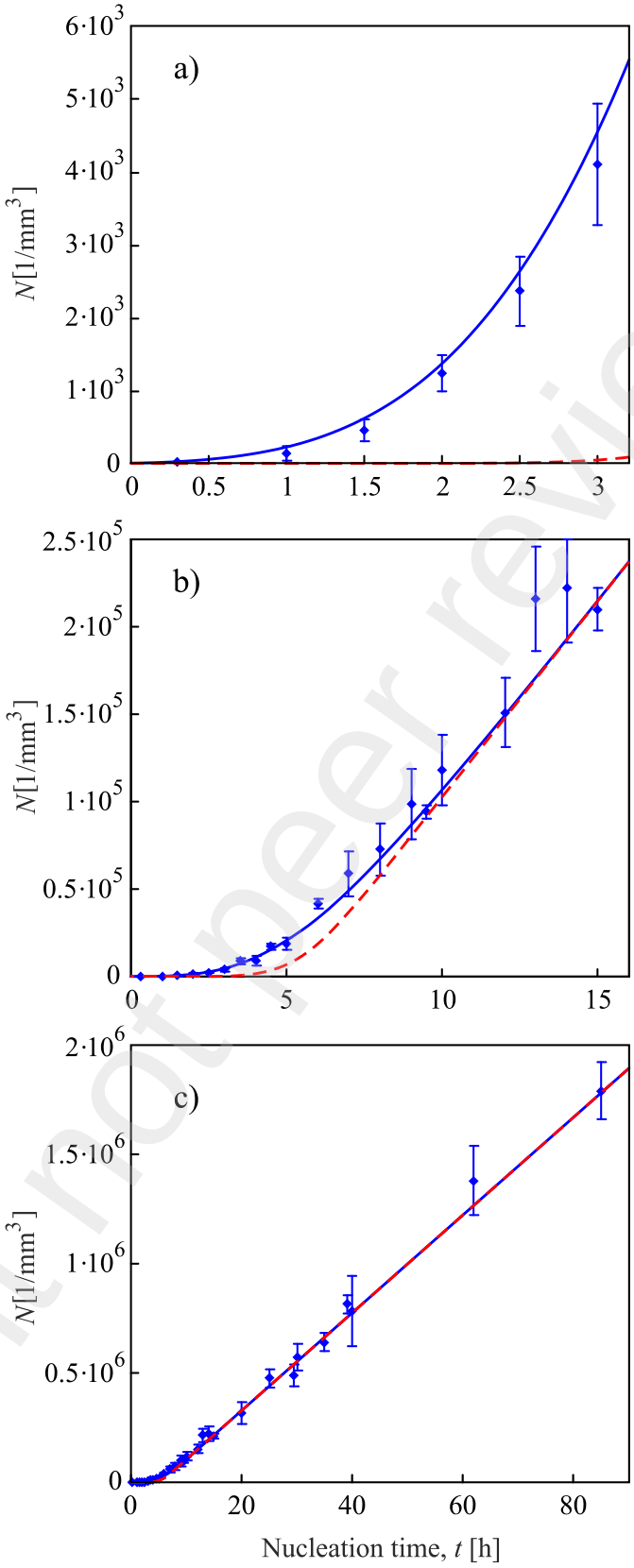

Fig. 5. Number of crystals per unit volume versus nucleation time at $T = 723\text{K}$ ($\sim T_g$) for different time intervals. The dashed red lines were obtained via simulations based on the cluster dynamics model with constant values of D and σ, which were fitting parameters to best describe the *final linear part* of the $N(t)$ curve shown in Fig. 5c. The blue solid line denotes a fit via (14), (17) and (18).

N versus *time* curves similar to those shown in Figs. 3-5 were also obtained for four temperatures (738, 746, 758, and 793K) above T_{max} and are shown by Figs. 6-8. The values of the nucleation rate at these 4 temperatures are very close to those obtained earlier for a lithium disilicate glass of another batch [5,20] (Fig. 14).

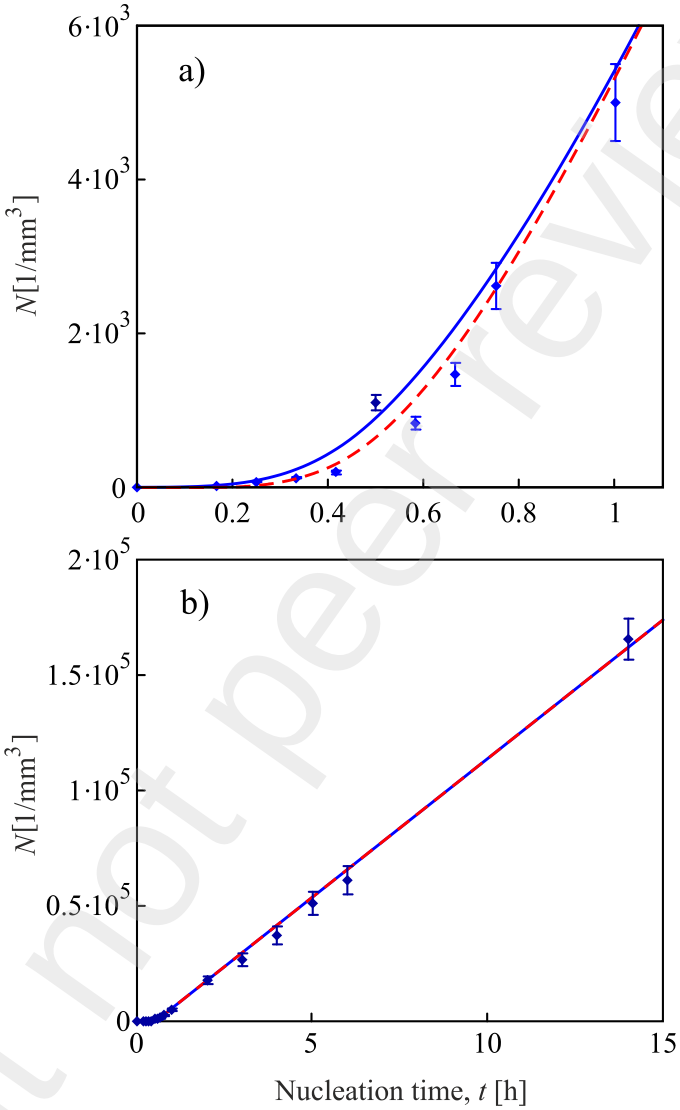

Fig. 6. Number of crystals per unit volume versus nucleation time at $T = 738$K for different time intervals. The blue solid line denotes a fit via Eqs. (14), (17) and (18), the dashed red lines were obtained via simulations based on the cluster dynamics model with constant D and σ, which were the fitting parameters that best describe the *final part* of the $N(t)$ curve shown in Fig. 6b.

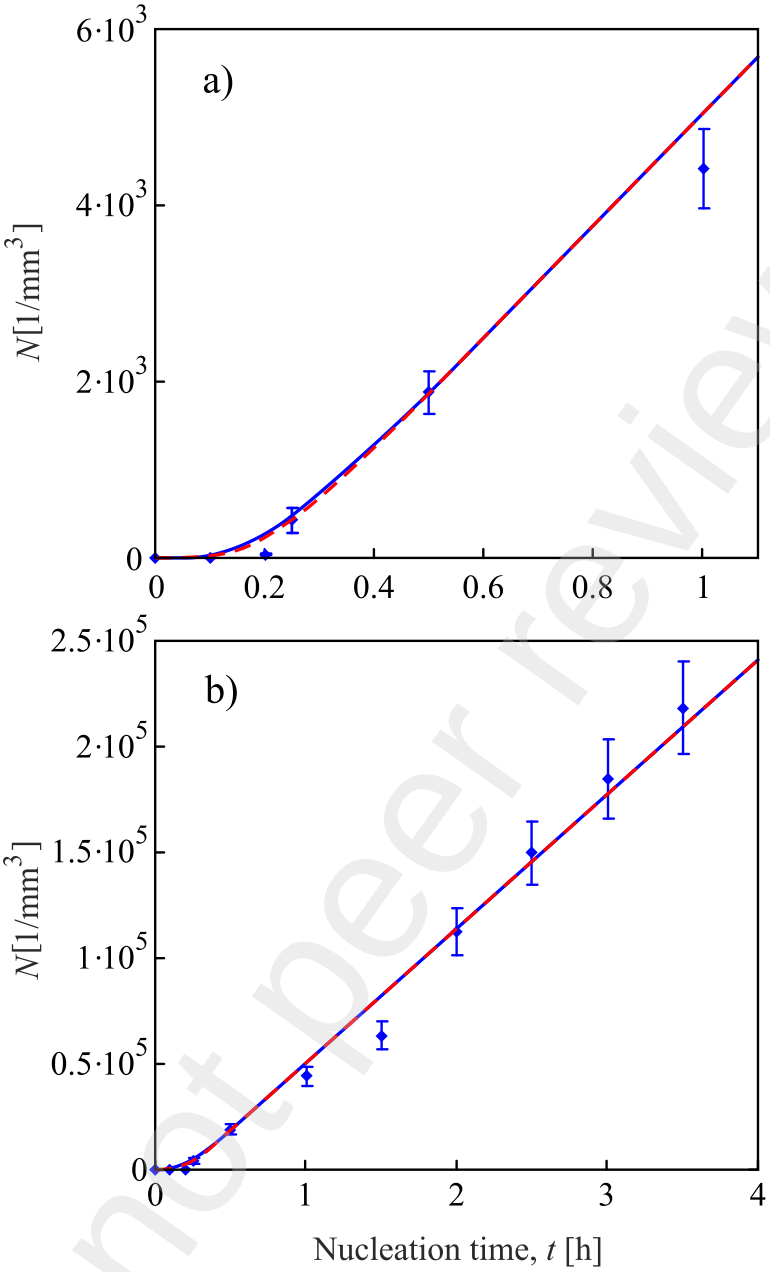

Fig. 7. Number of crystals per unit volume versus nucleation time at $T = 746$K for different time intervals. The blue solid line denotes a fit via Eqs. (14), (17) and (18), the dashed red lines were obtained via simulations based on the cluster dynamics model with constant D and σ, which were the fitting parameters that best describe the *final part* of the $N(t)$ curve shown in Fig. 7b.

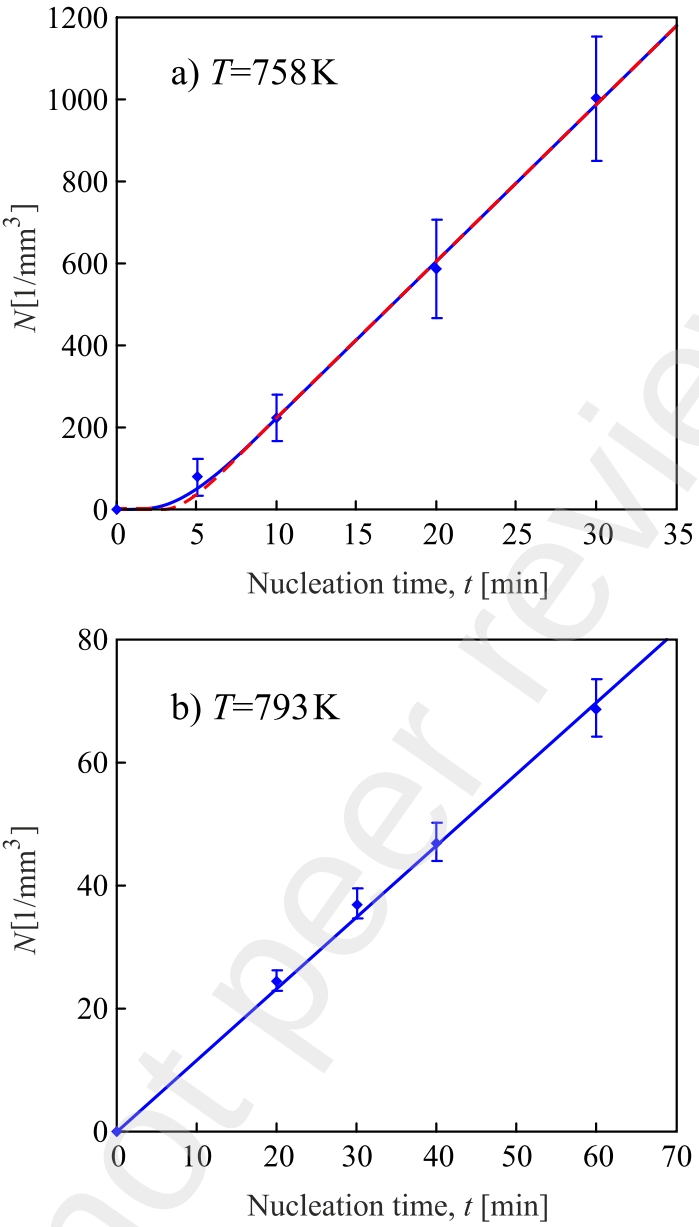

Fig. 8. Number of crystals per unit volume versus nucleation time at a) 758K and b) 793K. The blue solid line denotes a fit via Eqs. (14), (17) and (18), the dashed red lines in a) were obtained via simulations based on the cluster dynamics model with constant D and σ, which served as fitting parameters to best describe the *final part* of the $N(t)$ curve. In curve b) the two lines coincide for all treatment times.

4. Analysis and Discussion

4.1 Some basic equations of CNT

According to the CNT, at a given temperature and fixed state of the glass, a certain time-lag, τ_{ns}, is required to establish the steady-state distribution of clusters and resulting steady-state nucleation rate, I_{st}. Once it is established, this quantity remains constant, as long as the volume fraction of the crystalline phase remains sufficiently low to avoid interaction of the evolving

crystallites. The basic equations for the description of the steady-state nucleation rate, $I_{\rm st}$, and a time-lag, τ_{ns}, are [14,28,29]:

$$I_{st} = \frac{1}{d_0^3}\sqrt{\frac{\sigma}{kT}}\frac{2D}{d_0}\exp\left(-\frac{W_c}{k_B T}\right), \quad (1)$$

$$\tau_{ns} = \frac{16}{3}\frac{\sigma k_B T}{D d_0^2 \Delta G_{\rm v}^2}, \quad (2)$$

where $d_0 = 4.8$ nm is the effective size of the structural units, which is reasonably estimated as $d_0 \approx (V_{\rm M}/N_{\rm A})^{1/3}$ where $V_{\rm M}$ is the crystal molar volume, and $N_{\rm A}$ is Avogadro's number. $W_{\rm c}$ is the thermodynamic barrier for nucleation or the work of formation of a nucleus of critical size, R_c. For spherical nuclei, they are given by the following equations:

$$W_c = \frac{16}{3}\pi\frac{\sigma^3}{\Delta G_{\rm v}^2}, \quad (3)$$

$$R_c = \frac{2\sigma}{\Delta G_{\rm v}}. \quad (4)$$

In the above equations, T is the absolute temperature, D is the effective diffusion coefficient controlling nucleation, σ is the surface tension of the critical nucleus/melt interface, $k_{\rm B}$ is the Boltzmann constant, $\Delta G_{\rm v}$ is the change of the bulk contributions to the Gibbs free energy per unit volume of the crystal phase, i.e., the thermodynamic driving force for crystallization. Here we used the data of Takahashi and Yoshio [30] for the supercooled liquid and lithium disilicate crystal:

$$\Delta G_{\rm v}(T) = 8.40245024 \cdot 10^8 - 540266 \cdot T - 78.5116 \cdot T^2, \quad (5)$$

with T in Kelvin and $\Delta G_{\rm v}$ in J/m^3.

The introduction of a time-lag into the description of nucleation was first suggested by Zeldovich [31]. An overview on further developments of the theoretical description of the time-lag effect and its implications on nucleation can be found in [32].

4.2 Application to the interpretation of experimental data: General conclusions

In the current experiments, the situation is quite different as compared to the conventionally discussed cases that were sketched in Section 4.1. The number of crystals, N, versus time, t, dependences shown by Figs. 3-5 *cannot* be described by the $N(t)$ dependences obtained by numerical simulations based on the *cluster dynamics* model [14,33] with fixed system parameters; they are much more complex. For confirmation of the latter statement, we show the results of numerical computations by the dashed red lines in Figs. 3-5. These $N(t)$ dependences were obtained by (i) the numerical simulation taking D and σ as fit *constants* for a given nucleation temperature, and then (ii) the numerical simulation at the development temperature (this is particularly important for an appropriate description of the effect of the development method for

specification of the experimental nucleation data [26]). The effect of the cooling rate of the melt during the glass production and the heating rate to the development temperature on the cluster distributions and resulting $N(t)$ curves were taken into account in the simulation procedure (see details in **Supplementary materials**). Whereas, according to our estimates, the effect of finite heating rate from room temperature to the nucleation temperatures on the $N(t)$ dependences is very weak and, therefore, was ignored.

The following question then arises: at which time interval of the $N(t)$ dependence should the respective D and σ be determined? For the results shown in Figs. 3-5 by red dashed curves, these parameters were calculated from the best fits to the *final parts* of measured $N(t)$ data. It can be observed in these figures that the drawn curves do *not describe the preceding parts* of the $N(t)$ experimental dependencies, especially their beginning, where the calculated smooth red dashed curves are far below the experimental points. Moreover, vice-versa, one can fit the parameters D and σ from the initial stages, but then the final states cannot be appropriately described. Similarly, less explicit results are shown in Figs. 6-8 for temperatures above T_{max}.

The following important conclusions result from the above described experiments:

i. For any chosen nucleation temperature, above and below T_{max}, the *cluster dynamics* model cannot describe the $N(t)$-curves in the whole range of measurements using a single set of D and σ.

ii. The parameters, ΔG and σ, which determine the work of critical cluster formation, vary over time during the nucleation experiments.

iii. Thus, we assume that the observed change in these parameters is a consequence of glass relaxation, which strongly affects the nucleation rate.

As will be shown below, the evolution of the nucleation rate, dN/dt, mainly reflects the structural relaxation process of the glass and *not* the normal transient nucleation regime assumed by CNT.

4.3 The diffusion coefficient controlling nucleation

Any analysis of the nucleation process requires the knowledge of the effective diffusion coefficient and its temperature dependence. Supposing that the state of the glass is unchanged, the diffusion coefficient controlling nucleation has usually been determined via measurements of the nucleation time-lag, or directly as a fitting parameter in simulation methods. However, we have shown in the previous section that, at any temperature, the parameters determining the work of critical nucleus formation vary over time due to the glass relaxation. This result implies that the fitting procedure performed above (see dashed red lines in Figs. 3-8) is ***not correct*** because it does not take into account the evolution of these parameters during the period preceding the time

interval used for fitting. Thus, in this case it is not possible to determine the nucleation time-lags (of the CNT) and the corresponding diffusion coefficients using Eq. (2) from the experimental *N* vs *t* plots.

For this reason, in this article we follow another way of determining the diffusion coefficient, which relies on *crystal growth* rates. Here we use experimental crystal growth rates, $U(T)$, reasonably assuming that the nucleation and growth are governed by the same diffusion coefficient. The values of growth rates measured here for the studied glass at 703, 713 and 863K match very well to the literature data.

The growth rate in glass-forming liquids is approximately given by [28]

$$U = f\frac{D_U}{4d_0}\left[1 - \exp\left(-\frac{\Delta G_{\mathrm{v}} d_0^3}{k_B T}\right)\right]. \quad (6)$$

The thermodynamic term in Eq. (6) is very small at the temperatures of crystal nucleation and growth considered in this work, and henceforth we will neglect it. In addition, we will consider the normal growth mechanism ($f = 1$). The screw dislocation model assumes an even higher diffusion coefficient for a given (experimental) growth rate, and hence only reinforces our conclusion made in the next Section 4.4 that the nucleation time-lags are much smaller than the characteristic times of the long-term structural relaxation that is responsible for the evolution of the nucleation process. Therefore, the increased nucleation rate, dN/dt, mainly reflects the structural relaxation process of the glass and *not* the classical transient nucleation regime described by CNT.

The diffusion coefficients, D_U, estimated from Eq. (6) using the literature [34] and our own growth rate data are shown in Fig. 9 by filled and empty rhombuses, respectively. The solid blue lines represent Arrhenius fits for two temperature intervals

$$D_U = D_0 \exp\left(-\frac{E_D}{k_B T}\right), \quad (7)$$

for $T < 786$K

$$D_0 = 2.725 \cdot 10^5 \ \mathrm{m^2 s^{-1}}, \quad E_D = 5.944 \cdot 10^{-19}\mathrm{J}, \quad (8)$$

and for $T \geq 786$K

$$D_0 = 54.714 \ \mathrm{m^2 s^{-1}}, \quad E_D = 5.02 \cdot 10^{-19}\mathrm{J}. \quad (9)$$

For the sake of comparison, the diffusion coefficient D_η obtained by using the viscosity via the Stokes-Einstein-Eyring equation

$$D_\eta(T) = \frac{k_B T}{\kappa d_0 \eta(T)}, \quad (10)$$

is also shown in Fig. 9. The coefficient $\kappa = 0.35$ yields $D_\eta(T) = D_U(T)$ at high temperatures. Consequently, it is clear that in the system under consideration, diffusion (responsible for

aggregation processes in crystal nucleation and growth) and viscosity diverge at a temperature around 850K. This "decoupling" between D_η and D_U in glass-forming liquids is well-known [35].

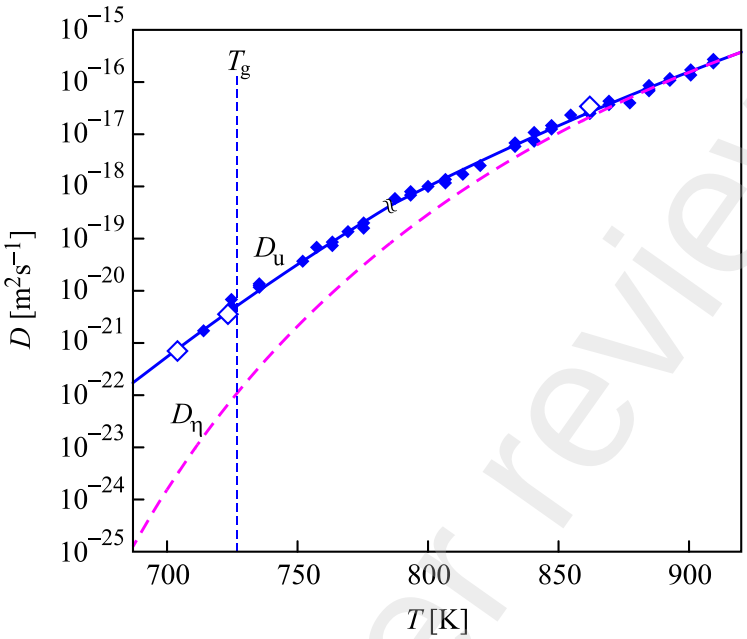

Fig. 9. Diffusion coefficients estimated from crystal growth rate, D_U (solid blue line, see Eqs. (7), (8), (9)), and viscosity D_η (dashed magenta line, see Eq.(10)). The filled and empty rhombuses refer to the literature and our growth rate data, respectively.

Using the diffusion coefficient, D_U, for the analysis of the nucleation kinetics is also supported by the following fact: as we showed above, the fitting procedure of the N vs t data within the framework of the CNT assumptions is not correct. However, this fitting could be valid if we used the very *beginning* of the N vs t dependence, before any sign of the relaxation process can be detected. Proceeding in such a way, we evaluate that at 703K the fitted nucleation diffusion coefficient D is very close to D_U.

4.4 Work of critical cluster formation and steady-state nucleation rates

Using a diffusion coefficient determined from growth rates results in a very important consequence for further analysis of the nucleation kinetics. According to Table 2, the nucleation time-lag, τ_{ns}, estimated by Eq.(2) using $D = D_U$ is shorter than the characteristic time of structural relaxation, τ_{sr} (Eqs. (19), (20)) by over *1-2 orders* of magnitude (Table 2).

In this case, a quasi-stationary nucleation regime establishes *much faster* than the state of glass changes, and continuously follows the relaxation process. Thus, this temporary steady-state nucleation rate, $I_{tst}(t)$, is determined by a simple analytical formula (Eq.1), again, however with a *time-dependent* work of the critical cluster formation determined by the current state of the glass.

In this case, the increase of nucleation rate mainly reflects the glass relaxation process, $I(t) \approx I_{tst}(t)$, because the classical transient nucleation can only be detected at the very beginning of the *N* vs *t* curves, where the effect of relaxation can be overlooked.

To take into account the effect of structural relaxation on the nucleation process, we introduce a structural order parameter, ξ, and assume that the thermodynamic driving force for crystallization, $\Delta G_{\rm v}$ is determined by the ratio $\zeta = \xi/\xi_e$ (ξ_e is the metastable equilibrium value of the structural order-parameter), by the following simple dependence:

$$\Delta G_{\rm v}(\zeta) = \Delta G_{\rm v,eq}\zeta. \qquad (11)$$

The semi-empirical Skapski-Turnbull equation was used to estimate the surface energy

$$\sigma(\zeta) = \frac{\alpha}{d_0^2}\Delta G_{\rm v}(\zeta) = \sigma_{eq}\frac{\Delta G_{\rm v}(\zeta)}{\Delta G_{\rm v,eq}} = \sigma_{eq}\zeta. \qquad (12)$$

A more detailed theory of the effect of structural relaxation on the nucleation process is given in [25].

In Eq. (12), we assumed that the value of the parameter α does not depend on ζ, the equilibrium value $\Delta G_{\rm v,eq}$ is determined by Eq. (5), and σ_{eq} may be described by Tolman's equation

$$\sigma_{eq}(T) = \frac{\sigma_0}{1+\frac{\delta}{R_c(T)}}, \qquad (13)$$

where σ_0 is the surface energy of a planar interface (macroscopic crystal), δ is the Tolman length, and $R_c(T)$ is determined by Eq. (4). It follows from Eqs. (4), (11), and (12), that the critical size, R_c, does not depend on the structural order parameter.

Eqs. (11), (12) yield the dependence of the work of critical cluster formation on the reduced structural order parameter ζ,

$$W_c(\zeta) = W_{c,eq}\zeta, \qquad (14)$$

where equilibrium value $W_{c,eq}$ is determined by Eq. (3).

Eqs. (1), (12) and (14) yield *a temporary steady-state* nucleation rate, $I_{tst}(T,t)$,

$$I_{tst}(T,t) = \frac{1}{d_0^3}\sqrt{\frac{\sigma_{eq}(T)\zeta(t)}{kT}}\frac{2D_U}{d_0}\exp\left(-\frac{W_{c,eq}(T)\zeta(t)}{k_BT}\right), \qquad (15)$$

where D_U is estimated from crystal growth rate, $U(T)$ (Eqs. (7), (8)), and the surface tension is given by Eq. (13) with

$$\sigma_0 = 0.191091\ \mathrm{J/m^2},\ \ \delta = 0.0828d_0. \qquad (16)$$

These data (σ_0 and δ) were obtained from a fitting procedure to achieve the best agreement with the experimental steady-state nucleation rates measured above T_{max}, at 738K, 746K, 758K and 793K, where the relaxation process finished quickly and $\zeta = 1$. These nucleation rates are

close to those reported in our previous measurements [5,7] for another batch of lithium disilicate glass, denoted by the green rhombus in Fig. 14.

Here we neglected the possible influence of the relaxation (order parameter) on the diffusion coefficient. We assumed that the activation barrier for diffusion is proportional to the glass density, and since glass densifies during the alpha relaxation period, the diffusion coefficient is expected to decrease over the alpha relaxation time. However, the change in density is relatively small ($e.g.,\sim 0.5\%$ for 703K, see Fig. 15 and Eq. (27)), hence its effect on diffusion was considered negligible. We are aware that this assumption requires experimental verification.

The evolution of the reduced structural order parameter, $\zeta(t)$, can be approximated by the Kohlrausch stretched exponent law:

$$\zeta(t) = 1 + \zeta_0 \cdot \exp\left[-\left(\frac{t}{\tau_{sr}}\right)^{\beta}\right]. \qquad (17)$$

Here ζ_0, τ_{sr} and β are fitting parameters to achieve the best agreement of the calculated $N(t)$ dependence

$$N(t) = \int_0^t I_{tst}(t')dt' \qquad (18)$$

with the experimentally measured curves. The fitting results are presented in Table 1, and the respective $N(t)$ curves are shown in Figs. 3-8 by solid blue lines.

Table 1. The fitting parameters ζ_0, τ_{sr} and β in Eq. (17) for different nucleation temperatures

T [K]	703	713	723	738	746	758
ζ_0	0.287	0.17	0.17	0.17	0.17	0.17
τ_{sr} [h]	61	10.3	2.2	0.235	0.085	0.018
β	0.65	1	1	1	1	1

The $\tau_{sr}(T)$ shown in Fig. 10 can be fitted with the following formulae

$$\tau_{sr}(T) = \varphi(T)\tau_\eta(T), \qquad (19)$$

where

$$\tau_\eta(T) = \frac{d_0^2}{D_\eta(T)} \qquad (20)$$

is a characteristic diffusion time from viscosity, and $\varphi(T)$ is the linear correction function

$$\varphi(T) = 10.319 - 0.012T.$$

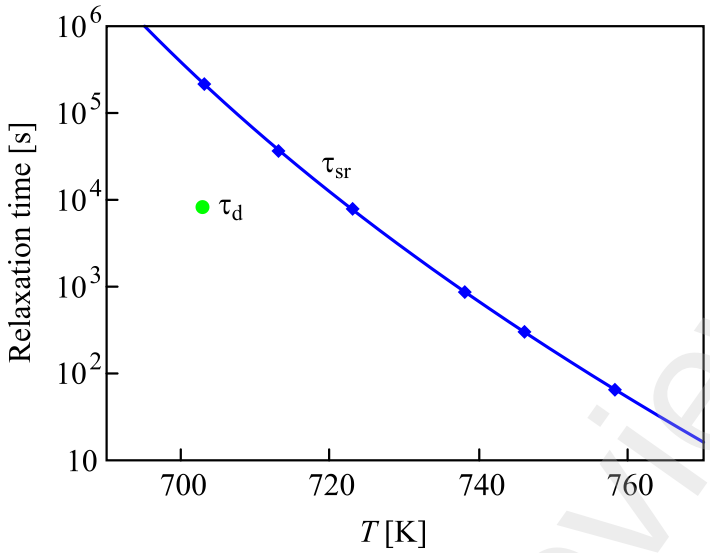

Fig. 10. Characteristic relaxation times versus temperature: rhombuses denote the characteristic times of the long-term structural relaxation responsible for the evolution of the nucleation process, τ_{sr} (see Eq. (17)), whereas the solid line denotes the characteristic time of structural relaxation calculated from the viscosity by Eq. (19), and the circle is the characteristic time of density relaxation, τ_d (see Eq. (27)).

Fig. 10 shows a strong correlation between these two characteristic times, $\tau_{sr}(T)$ and $\tau_\eta(T)$. This correlation indicates that the viscosity determines the long-term structural relaxation responsible for the evolution of the nucleation process, resulting in increased nucleation rate after the end of alpha relaxation (as measured by the evolution of the glass density with time).

The evolution of the work of critical cluster formation (Eq. (14)) and corresponding nucleation rate (Eq. (15)) at 723K and 703K are presented by Fig. 11 and Fig.12a, respectively. The work of critical cluster formation decreases and the temporary nucleation rate increases over time.

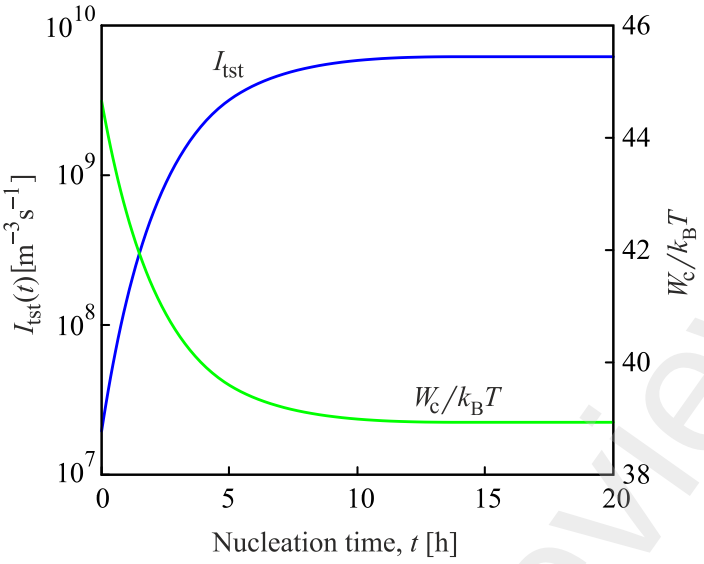

Fig. 11. Evolution of the nucleation rate (Eq. (15)) and the work of critical nucleus formation (Eq. (14)) for $T = 723$K as a function of nucleation time (see text for details).

However, using a traditional relaxation function ignores the intriguing feature of the $N(t)$ for $T = 703$K dependence: it reveals several parts with constant slopes, i.e. several time intervals corresponding to constant nucleation rates (Fig. 3).

The reduced structural order parameter $\zeta(t)$ for these time intervals with constant nucleation rates are given by

$$\zeta_{1\dots6} = 1.259, 1.182, 1.111, 1.046, 1.016, 1. \quad (21)$$

Eq. (15) yields the respective temporary steady-state nucleation rates at the steps:

$$I_{tst,1\dots6} = (0.00028, 0.0042, 0.073, 0.84, 2.63, 4.72) \cdot 10^9 \text{ m}^{-3}\text{s}^{-1}. \quad (22)$$

To describe the transient behavior between the different stages, we used the following step function with linear transitions between the steps:

$$\zeta(t) = \begin{cases} \zeta_1 \text{ for } t \le t_{r,1} \\ \zeta_i + \dfrac{\zeta_{i+1} - \zeta_i}{t_{s,i} - t_{r,i}}\left(t - t_{r,i}\right) \text{ for } t_{r,i} < t \le t_{s,i}, \quad i = 1 \dots 5 \\ \zeta_{i+1} \text{ for } t_{s,i} < t \le t_{r,i+1}, \quad i = 1 \dots 4 \\ \zeta_6 \text{ for } t > t_{s,5} \end{cases} \quad (23)$$

where

$$t_{r,1\dots5} = 5, 33, 80, 210, 500 \text{ h} \quad (24)$$

is the time of the beginning of the relaxation process from one to another step,

$$t_{s,1\dots5} = 13, 45, 115, 260, 560 \text{ h} \quad (25)$$

is the time of the end of relaxation process, which is the beginning of the new step.

These parameters were used to fit the dependence $N(t)$ calculated by Eqs. (15) and (18) with the experimentally measured $N(t)$ dependence shown in Fig. 3. The magenta dashed dotted

line in Fig. 3 corresponds to this step function. The stepwise evolution of W_c and I_{ist} is shown in Fig. 12b.

It should be noted that the step function describes the experimental data for 703K better than the smooth approximation, especially for the initial part of the $N(t)$ dependence.

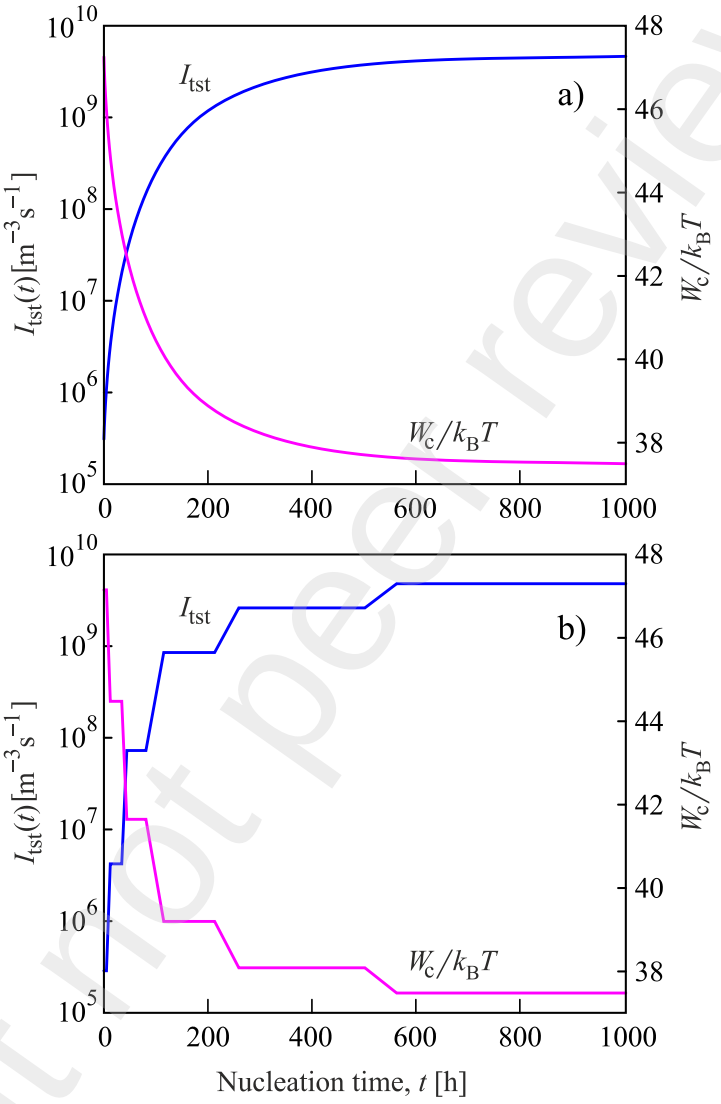

Fig. 12. Smooth (a) and stepwise (b) evolution for $T = 723$K ($\sim T_g$) of the work of critical nucleus formation (Eq. (14)) and respective nucleation rate (Eq.1) corresponding to dashed-dotted magenta and blue solid lines in Fig. 3, respectively.

Understanding the unusualness of stepwise relaxation, which contradicts the generally accepted concept of continuous relaxation, we present some considerations in its favor below.

In Fig. 13, a schematic illustration is given for the possible interpretation of the stepwise nature of the relaxation process, and hence of nucleation kinetics observed at $T = 703$K. At the glass transition, the supercooled liquid is transferred by cooling into a thermodynamically non-

equilibrium state, the glassy state (Fig. 13a). At temperatures below the glass transition temperature, relaxation (aging) takes place spontaneously. A mechanical analogy of this kind of behavior was illustrated by considering the motion of a solid particle under a force field (see [28]). This picture has been extended in [36] accounting for the potential energy landscape model of glass-forming systems, as advanced by Goldstein [37]. According to Goldstein, the highly viscous glass may be trapped for some time in local minima of the potential energy landscape. Perhaps this behavior is related to the known, but still scarcely studied phenomenon of liquid-liquid transition (polyamorphism) with changing external parameters [38-40]. However, in our case the supposed various liquid states are metastable with a limited lifetime.

These potential energy minima are denoted in Fig. 13b by the numbers 1-6. Note that the nucleation-growth process occurs simultaneously with structural relaxation, bringing the liquid into the thermodynamically stable crystalline phase. These processes are shown schematically in Fig. 8b: the system exists in the metastable state 3 in the time range $t_{s,2} < t < t_{r,3}$ (45…80 hours, see Fig. 3c) and transfers partially into a crystalline phase due to nucleation. From this metastable state 3 in the time range $t_{r,3} < t < t_{s,3}$ (80…115 hours), the system transfers into the lower metastable state 4 (see Fig. 3d) due to relaxation. This relaxation process results in an approach of the metastable state of the supercooled liquid denoted in Fig. 13b by the number 6, where the definitive steady-state nucleation regime is reached.

Thus, we identify the lifetimes of the glass towards the supercooled liquid at these local minima with time intervals corresponding to the constant nucleation rates observed in the experiments at 703K. The system can escape from these local minima only by stochastic thermal fluctuations. The intensity of such fluctuations increases with increasing temperature, and also the potential energy surface can be expected to become smoother. For this reason, it can be expected that the number of local minima and the duration the liquid is trapped in them decreases with increasing temperature. Therefore, at $T \geq 713$K we see a rather smooth $N(t)$ dependence.

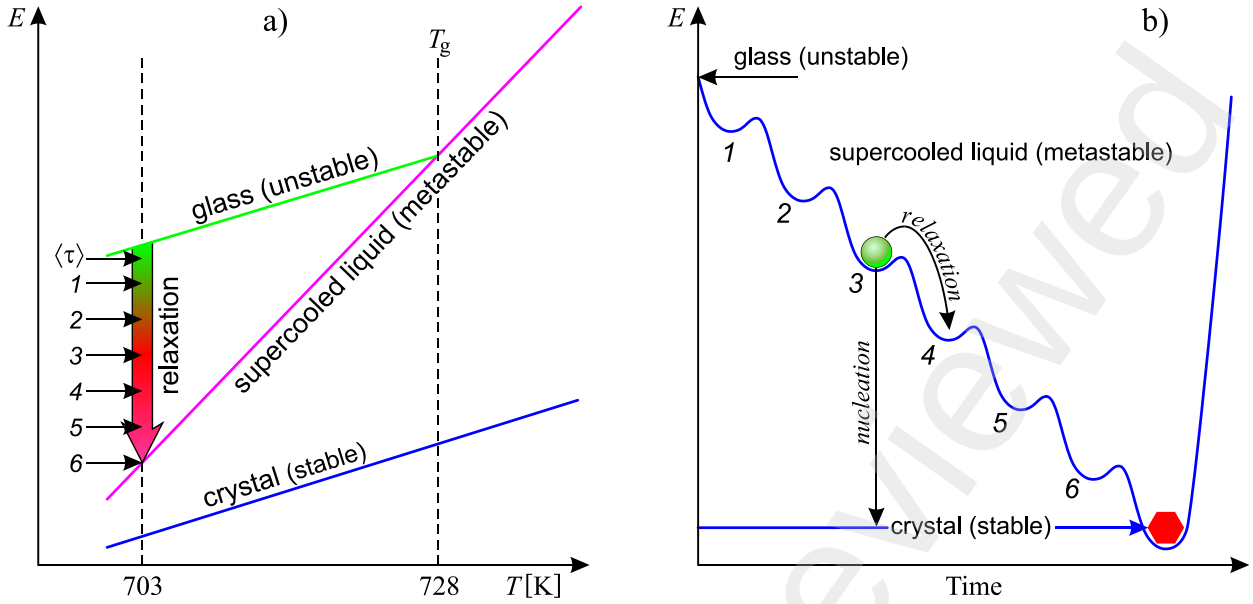

Fig. 13. Schematic illustrations of the energy of the crystal, supercooled liquid, and glass versus temperature (a) and relaxation of the later at a temperature below the glass transition (b).

The above model is hypothetical and, of course, needs to be expanded both by nucleation experiments and use of direct structural methods.

4.5 Effect of structural relaxation on nucleation and connection with the apparent "breakdown" of CNT at $T < T_{max}$

Fig. 14 summarizes the nucleation rate data showing the temperature dependence of the steady-state nucleation rate, I_{st}, corresponding to the equilibrium supercooled lithium disilicate melt and its evolution during glass annealing. The solid blue line is plotted via Eq. (1) with D estimated from crystal growth rate, $U(T)$, by Eqs. (7), (8) and a relation for the temperature dependence of the surface tension $\sigma_{eq}(R_c(T))$ given by Eq. (13).

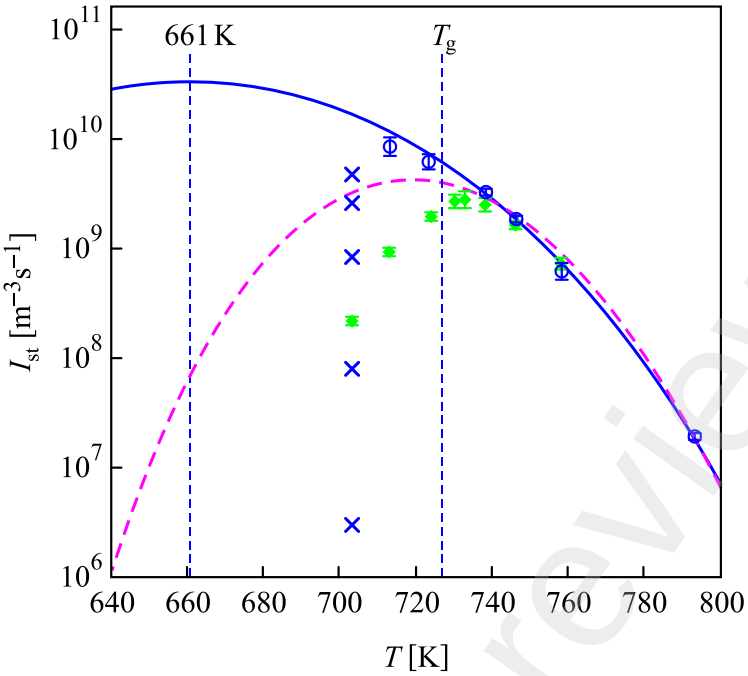

Fig. 14. Ultimate steady-state nucleation rates (blue circles). The crosses show the evolution (increase) of the nucleation rate over time at 703K Eq. (22), and the green rhombus shows our previous results [5] obtained for a LS2 glass of another batch, which did not reach a definitive steady-state below T_{max}. The blue solid line is the fitted CNT equation using *growth rate* data to calculate $D(T)$, which predicts a maximum $I_{st} \approx 3.2 \cdot 10^{10}\mathrm{m}^{-3}\mathrm{s}^{-1}$ at 661K (well-below the experimental maximum so far reported at ~733K). The magenta dashed line is plot with $D(T)$ calculated via viscosity.

The crosses in Fig. 14 denote the nucleation rates at $T = 703\mathrm{K}$ corresponding to the stepwise evolution of the nucleation rate shown in Fig. 12b. It is clearly seen that the nucleation rate increases with time, approaching the expected definitive value corresponding to $T = 703\mathrm{K}$.

The circles show the nucleation rates at temperatures 713, 723, 738, 746, 758 and 793K, corresponding to the final part of the corresponding dependences *N* vs *t*, which is very close to the theoretically expected values.

At first glance, it may seem that dependences $I_{st}(T)$ plotted using the diffusion coefficient, D_η, estimated from viscosity describe the experimental data. However, this conclusion is erroneous, because using D_η, allows us to describe only the slope of the final part of the $N(t)$ dependence, i.e., I_{st}, but not the actual $N(t)$ dependence.

We attribute the above described behavior to a very long relaxation processes in the glass that finally leads to its transition to a metastable (relative to the crystalline phase) supercooled liquid (see Fig. 13).

Previous measurements [5, 7] were restricted by nucleation times that were not long enough to reach glass stabilization at $T < T_{max}$. As a rule, when performing nucleation rate measurements well below T_g, most researchers stopped extending the nucleation time when the last part of the *N* vs *t* dependence could be considered linear. This can be considered as indirect evidence that different authors determined the nucleation rate corresponding to different steps similar to those observed in this work for $T = 703$K.

Thus, below the glass transition temperature, crystal formation starts first in a non-equilibrium *glassy* state and continues in non-stable and then metastable supercooled liquid as illustrated by the scheme in Figure 13a.

4.6 Characteristic relaxation times

To complete our analysis of the kinetics of nucleation, we also evaluated the structural relaxation kinetics of this glass. For the sake of comparison, we estimated the characteristic relaxation times and the times of the appearance of the first supercritical crystal in a given volume for the studied temperatures listed in Table 2. We referred to this table in Section 4.4 to justify the use of Eq. (1) for the nucleation rate.

Table 2. Different characteristic times: $\langle\tau\rangle$= the times of the appearance of the first supercritical crystal in a volume of 10 mm^3 Eq. (26); τ_{ns} = time-lag for nucleation Eq. (2); τ_{sr} = the characteristic time of structure relaxation Eq. (17).

T[K]	$\langle\tau\rangle$ [s]	τ_{ns} [s]	τ_{sr} [s]	$\tau_{sr}/\langle\tau\rangle$	τ_{sr}/τ_{ns}
703	591	354	219600	372	620
713	148	141	37080	250	262
723	75.7	70,6	7920	105	112
738	23.6	20.6	846	36	41
746	11.8	11.4	295	25	25.8
758	5.18	4.77	65	13	14

To a good approximation, the average time of formation of the first supercritical nucleus, $\langle\tau\rangle$, can be expressed as [30]

$$\langle\tau\rangle \cong \tau_{ns} + \frac{1}{I_{st}V}\,. \qquad (26)$$

Here I_{st} is the steady-state nucleation rate and V is the volume of the system. For the temperature range of interest near the glass transition temperature interval, the time of formation of the first supercritical nucleus for the volume of laboratory sample ($V = 10$ mm^3) is widely determined by

the nucleation time-lag, $\langle\tau\rangle \sim \tau_{ns}$ (see Table 2). For these computations, we are utilizing the diffusion coefficient, D_U, estimated from growth rates, Eq. (6), and the surface tension obtained from Eqs. (12) and (16).

Taking into account, that $\tau_{sr}/\tau_{ns} \gg 1$, we consider τ_{sr} as the characteristic time of the long relaxation responsible for the evolution of nucleation rate. This is the reason why the theoretical analysis of the experimental data assuming given fixed values of the parameters of liquid phase *cannot* describe the kinetics of nucleation. The time-dependence of the $N(t)$ curve is *not* a particular form of transient nucleation in the sense of Zeldovich [31,33], instead it is a consequence of variations of the state of the glass. According to Table 2, the ratio τ_{sr}/τ_{ns} decreases with increasing temperature reflecting in such way its approach to the temperature of decoupling between the growth rates and viscosity. However, a significant convergence of these characteristic times will occur at high temperatures corresponding to very low nucleation rates. The results discussed above suggest an evolution of the nucleation process, which is determined mainly by the relaxation of the glass towards the metastable supercooled liquid that occurs simultaneously with the nucleation process.

Let us note as well that τ_{sr} is much longer than the alpha-relaxation, which are estimated by the change of glass density, τ_d, shown in Fig. 15 and described by Eq. (27).

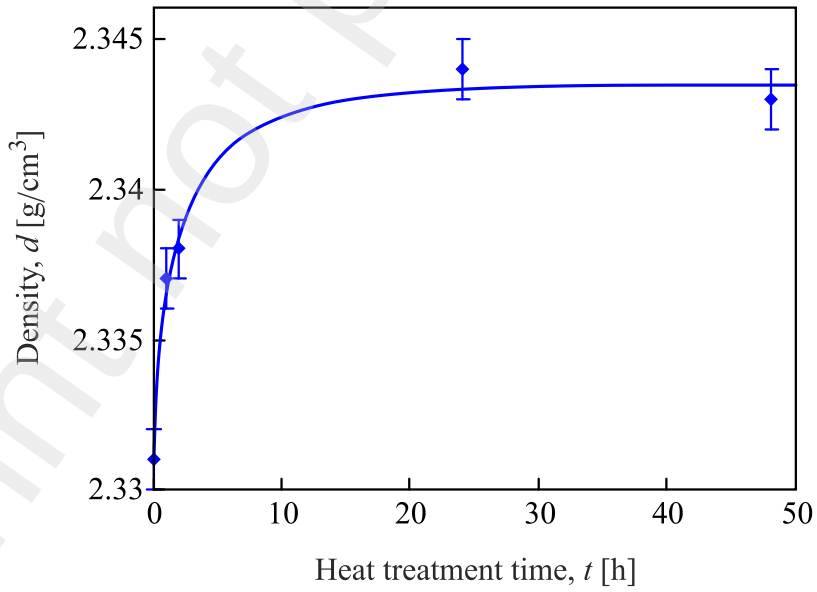

Fig. 15. Variation of density versus treatment time at $T = 703$K. The blue solid line is plotted by Eq. (27).

The variation of density versus treatment time at $T = 703$K can be approximated by the Kohlrausch stretched exponent law:

$$d(t) = 2.3435 - 0.0125\exp\left[-\left(\frac{t}{\tau_d}\right)^{0.615}\right], \qquad (27)$$

$$\tau_d = (2.33 \pm 0.48)[\text{h}].$$

It should be especially noted that after the alpha relaxation process that determines the density increase at 703K has practically terminated, the nucleation rate still increases by about 70 times until reaching its definitive steady-state regime. This fact is consistent with Goldstein's [37] idea that a liquid is still changing its structure even when its density no longer changes.

5. Final remarks

This work was stimulated by the long-standing, but not yet fully resolved problem of the alleged "breakdown" of CNT at low temperatures below T_{max} (for lithium disilicate glass T_{max} ~T_g). In that range, theoretical calculations (extrapolated from high temperature nucleation data) predict nucleation rates much higher than the measured values. This discrepancy between theory and experiment was reported for several glasses [9-14] and increases with decreasing temperature, achieving several orders of magnitude.

Our extensive prolongation of experimental studies of the N vs t dependencies in comparison with previously used treatment times for LS2 glass, and their analysis by numerical simulations based on the *cluster dynamics* model, show that the full $N(t)$ curve *cannot* be described by CNT with a single, unchanged set of the parameters σ and D.

Calculation of the nucleation time-lags, τ_{ns}, using the diffusion coefficient obtained from crystal growth rates, D_U, showed that at each moment of time, *a temporary quasi-stationary nucleation regime* is established. We stress that using D_U to analyze nucleation kinetics is a reasonable approximation, since nucleation and crystal growth are interrelated. Moreover, we showed that simulation of the initial part of the $N(t)$ dependence yields a diffusion coefficient, D, estimated as a fit parameter of the *cluster dynamic*s model, very close to D_U.

As the nucleation time decreases, this fitting procedure becomes more correct, since neglecting glass relaxation becomes more justified. Hence, a single set of the system parameters could be applied only to the description at the very beginning of the nucleation process. On the other hand, in the advanced stage, the $N(t)$ dependence reflects the glass relaxation process and not the conventional transient nucleation described by CNT. This finding applies for both high ($T > T_{max}$) and low ($T < T_{max}$) temperatures. The difference lies only in the fact that at $T > T_{max}$ the relaxation time is too short if compared with the experimental time, and, therefore, most of the $N(t)$ dependence refers to the definitive steady-state nucleation rate in the metastable supercooled liquid.

Thus, our experiments and their interpretation showed that the "breakdown" of CNT at low temperatures results from very slow glass relaxation, which exceeds the conventional alpha-relaxation process (e.g., measured by density evolution). After this period, the nucleation rate continues to approach its definitive steady-state nucleation rate, corresponding to the fully relaxed glass that finally reached the SCL state. Then, the experimental rates agree with the theoretically expected values (extrapolated from temperature above T_g). In other words, the previously reported breakdown of CNT was based on nucleation rate data that did *not* refer to the fully relaxed glass.

6. Summary and Conclusions

We carried out very long heat treatments (up to 2,212 hours) below the laboratory glass transition temperature of a lithium disilicate glass, and analyzed the experimental N versus time curves with a *cluster dynamics* model. Thus, we discovered several *new* findings: i) Significant prolongation of the heat treatment time at temperatures below T_g leads to an increase of the nucleation rate until it reaches the theoretically expected steady-state value. This variable nucleation rate is *not* a particular form of transient nucleation in the sense proposed by Zeldovich (transient nucleation occurs only in the very beginning of the N vs t curves, since the relaxation process can be neglected). ii) At any given temperature, the evolution of the crystal number density on nucleation time *cannot* be described by CNT using a single set of diffusivity and interfacial energy. Since these parameters depend on the state of glass, we reasonably assume that the evolution (increase) of the nucleation rates with time is mainly determined by the long structural relaxation mode of the glass towards the metastable supercooled liquid, which occurs simultaneously with the nucleation process.

Finally, the most important finding of this work is that the characteristic time of this relaxation mode determining nucleation kinetics is *much longer* than that of the traditional alfa-relaxation process estimated by the temporal change of the glass density. Therefore, the previously reported breakdown of CNT was based on nucleation rate data that did *not* refer to the *definitive* steady-state regime corresponding to a fully relaxed glass that finally reached the SCL state.

Our original results shed light on the significant effect of structural relaxation on crystal nucleation and pave the way for further experimental and theoretical work.

Acknowledgements

We are thankful to CNPq, the São Paulo Research Foundation - FAPESP Project # 2013/007793-6, and CAPES Project # 88887.468838/2019-00 for funding this research.

References

[1] J.M.F. Navaro, El Vidrio, CSIC, Madrid, Spain, 1991

[2] W. Höland, G. Beall, Glass-Ceramic Technology, American Ceramic Society, 2002.

[3] J.W. Christian, The Theory of Transformation in Metals and Alloys, Part I, Pergamon, Oxford, (1981).

[4] K.F. Kelton, A.L. Greer, Nucleation in condensed matter. Applications in Materials and Biology, Pergamon Mater. Series (2010) 276.

[5] V.M. Fokin, A.M. Kalinina, and V. N. Filipovich, Nucleation in silicate glasses and effect of preliminary heat treatment on it, J. Cryst. Growth 52 (1981) 115–121. https://doi.org/10.1016/0022-0248(81)90178-0

[6] A.S. Abyzov, V.M. Fokin, N.S. Yuritsyn, A.M. Rodrigues, J.W.P. Schmelzer, The effect of heterogeneous structure of glass-forming liquids on crystal nucleation, J. Non-Crystalline Solids 462 (2017) 32–40. http://dx.doi.org/10.1016/j.jnoncrysol.2017.02.004

[7] M.L.F. Nascimento, V.M. Fokin, E.D. Zanotto, A.S. Abyzov, Dynamic processes in a silicate liquid from above melting to below the glass transition, J. Chem. Phys. 135 (2011) 194703/1-18. doi: 10.1063/1.3656696

[8] A.M. Kalinina, V.N. Filipovich, V.M. Fokin, Stationary and non-stationary crystal nucleation rate in a glass of $2Na_2O.CaO.3SiO_2$ stoichiometric composition, J. Non-Crystalline Solids 38&39 (1980) 723–728. doi:10.1016/0022-3093(80)90522-0

[9] A.S. Abyzov, V.M. Fokin, A.M. Rodrigues, E.D. Zanotto, J.W.P. Schmelzer, Effect of elastic stress on the thermodynamic barrier for crystal nucleation, J. Non-Crystalline Solids 432 (2016) 325–333. doi: 10.1016/j.jnoncrysol.2015.10.029

[10] V.M. Fokin, A.S. Abyzov, E.D. Zanotto, D.R. Cassar, A. M.Rodrigues, J.W.P. Schmelzer, Crystal nucleation in glass-forming liquids: Variation of the size of the "structural units" with temperature, J. Non-Crystalline Solids 447 (2016) 35–44. http://dx.doi.org/10.1016/j.jnoncrysol.2016.05.017

[11] P.K. Gupta, D.R. Cassar, E.D. Zanotto, Role of dynamic heterogeneities in crystal nucleation kinetics in an oxide supercooled liquid, J. Chem. Phys. 145 (2016) 211920/1–211920/8. https://doi.org/10.1063/1.4964674

[12] D.R. Cassar, A.H. Serra, O. Peitl, E.D. Zanotto, Critical assessment of the alleged failure of the Classical Nucleation Theory at low temperatures, Journal of Non-Crystalline Solids 547 (2020) 120297. doi:10.1016/j.jnoncrysol.2020.120297.

[13] X. Xia, D.C. van Hoesen, M.E. McKenzie, R.E. Youngman, and K.F. Kelton, The Low-Temperature Nucleation Rate Anomaly in Silicate Glasses is an Artifact, arXiv.org>cond-mat>arXiv:2005.04845.

[14] A.S. Abyzov, J.W.P. Schmelzer, V.M. Fokin, and E.D. Zanotto, Crystallization of supercooled liquids: Self-consistency correction of the steady-state nucleation rate, Entropy 22, 558/1-28 (2020); doi:10.3390/e22050558.

[15] J.W.P. Schmelzer and C. Schick, General concepts of crystallization: Some recent results and possible future developments. In: Advances in Dielectrics Series (F. Kremer, series editor): Dielectrics and Crystallization (T.A. Ezquerra, A. Nogales, Eds.), Springer, in press.

[16] G. Johari and J.W.P. Schmelzer, Crystal Nucleation and Growth in Glass-forming Systems: Some New Results and Open Problems. In: J. W. P. Schmelzer (Editor), Glass: Selected Properties and Crystallization (de Gruyter, Berlin, 2014, pp. 521-585).

[17] J.W.P. Schmelzer and A.S. Abyzov, Crystallization of glass-forming melts: New answers to old questions, J. Non-Crystalline Solids, 501, 11-20 (2018). doi:10.1016/j.jnoncrysol.2017.11.047.

[18] J.W.P. Schmelzer and C. Schick, Dependence of Crystallization Processes of Glass-forming Melts on Prehistory: A Theoretical Approach to a Quantitative Treatment, Physics and Chemistry of Glasses, European Journal of Glass Science and Technology B 53, 99-106 (2012).

[19] C. Schick, E. Zhuravlev, R. Androsch, A. Wurm, and J.W.P. Schmelzer, Influence of Thermal Prehistory on Crystal Nucleation and Growth in Polymers. In: J.W.P. Schmelzer (Editor), Glass: Selected Properties and Crystallization (de Gruyter, Berlin, 2014, pp. 1-93).

[20] V.M. Fokin, E.D. Zanotto, N.S. Yuritsyn, and J.W.P. Schmelzer, Homogeneous Crystal Nucleation in Silicate Glasses: A Forty Years Perspective, J. Non-Crystalline Solids 352, 2681-2714 (2006). doi: 10.1016/j.jnoncrysol.2006.02.074.

[21] C. Schick, R. Androsch, and J.W.P. Schmelzer, Topical Review: Homogeneous crystal nucleation in polymers, J. Phys.: Condens. Matter 29, 453002/1-35 (2017).

[22] V.M. Fokin, E.D. Zanotto, and J.W.P. Schmelzer, Homogeneous Nucleation versus Glass Transition Temperature, J. Non-Crystalline Solids 321, 52-65 (2003). doi: 10.1016/S0022-3093(03)00089-9.

[23] A.S. Abyzov, V.M. Fokin, E.D. Zanotto, Predicting homogeneous nucleation rates in silicate glass-formers, J. Non-Crystalline Solids. 500 (2018) 231–234. https://doi.org/10.1016/j.jnoncrysol.2018.08.002

[24] J.W.P. Schmelzer, A.S. Abyzov, V.M. Fokin, C. Schick, and E.D. Zanotto, Crystallization in glass-forming liquids: Effects of fragility and glass transition temperature, J. Non-Crystalline Solids 428, 68-74 (2015). doi: 10.1016/j.jnoncrysol.2015.07.044

[25] J.W.P. Schmelzer, T.V. Tropin, V.M. Fokin, A.S. Abyzov and E.D. Zanotto, Effects of glass transition and structural relaxation on crystal nucleation: Theoretical description and model analysis, Entropy, DOI: 10.20944/preprints202008.0719.v1.

[26] G. Tammann, Über der Abhängigkeit der Zahlt der Kerne, welche sich in verschiedenen unterkühlten Flüssigkeiten bilden, von der Temperatur, Z. Phys. Chem. 25 (1898) 441-479.

[27] R.T. DeHoff, Quantitative Microscopy, McGraw-Hill Book Company, 1968.

[28] I.S. Gutzow, J.W.P. Schmelzer, The Vitreous State: Thermodynamics, Structure, Rheology, and Crystallization, 1st ed., Springer, Berlin, 1995 Second enlarged edition, Springer, Heidelberg, 2013.

[29] D. Kashchiev, Solution of the non-steady state problem in nucleation kinetics, Surf Sci. 14 (1969) 209–220.

[30] K. Takahashi, T. Yoshio, Thermodynamic quantities of alkali silicates in the temperature range from 25℃ to melting point, Yogyo-Kyokai-Sch 81 (1973) 524–533.

[31] Y.I. Frenkel, The Kinetic Theory of Liquids, Oxford University Press, Oxford, 1946.

[32] J.W.P. Schmelzer, A.S. Abyzov, V.G. Baidakov, Time of formation of the first supercritical nucleus, time-lag, and the steady-state nucleation rate, International Journal of Applied Glass Science, 2017; 8: 48–60 DOI: 10.1111/ijag.12243

[33] K.F. Kelton, A.L. Greer, and C. V. Thompson, Transient nucleation in condensed systems, J. Chem. Phys. 79 (1983) 6261-6276; doi: 10.1063/1.445731

[34] SciGlass - Glass Property Information System (http://www.sciglass.info)

[35] J.W.P. Schmelzer, A.S. Abyzov, V.M. Fokin, C. Schick, E.D. Zanotto, Crystallization in glass-forming liquids: Effects of decoupling of diffusion and viscosity on crystal growth, J. Non-Crystalline Solids, 429 (2015) 45-53. doi:10.1016/j.jnoncrysol.2015.08.027

[36] I. Gutzow, V. Yamakov, D. Ilieva, Ph. Babalievski, and L. D. Pye, Generic Phenomenological Theory of Vitrification, Glass Physics and Chemistry, 27 (2001) 148–159. https://doi.org/10.1023/A:1011384427512.

[37] M. Goldstein, Viscous Liquids and the Glass Transition: A Potential Energy Barrier Picture, J. Chem. Phys. 51, 3728 (1969); doi: 10.1063/1.1672587

[38] V. Lubchenko and P.G. Wolynes, Theory of Aging in Structural Glasses, J. Chem. Phys. 121 (2004) 2852–2865; https://doi.org/10.1063/1.1771633

[39] P.F. McMillan, Polyamorphic transformations in liquids and glasses, J. Mater. Chem., 14 (2004) 1506–1512 https://doi.org/10.1039/B401308P

[40] P.K. Hung, N.T. Nhan, Polyamorphism in the silica glass, Scripta Materialia 63 (2010) 12–15 https://doi.org/10.1016/j.scriptamat.2010.02.036